

## Using Two Fluorescent Probes to Dissect the Binding, Insertion, and Dimerization Kinetics of a Model Membrane Peptide

Jia Tang,<sup>†</sup> Hang Yin,<sup>‡,§</sup> Jade Qiu,<sup>‡</sup> Matthew J. Tucker,<sup>†</sup> William F. DeGrado,<sup>†,‡</sup> and Feng Gai<sup>\*†</sup>

*Department of Chemistry and Department of Biochemistry and Biophysics, University of Pennsylvania, Philadelphia, Pennsylvania 19104, and Department of Chemistry and Biochemistry, University of Colorado, Boulder, Colorado 80309*

Received November 17, 2008; E-mail: gai@sas.upenn.edu

While the study of how globular proteins fold has reached an advanced stage, there have been far fewer studies focused on the folding dynamics of membrane proteins.<sup>1–4</sup> This is due in part to the fact that most membrane proteins are insoluble in aqueous solution, thus making kinetic studies (e.g., via mixing) difficult. Here we show that through the use of a water-soluble transmembrane (TM) peptide, anti- $\alpha_{IIb}$ ,<sup>5,6</sup> and two fluorescent probes, tryptophan (Trp) and *p*-cyanophenylalanine (Phe<sub>CN</sub>), it is possible to kinetically dissect distinct phases in the peptide–membrane interaction, representing binding, insertion, and dimerization, thus providing new mechanistic and kinetic information on several processes that are fundamentally important to membrane protein folding.

Anti- $\alpha_{IIb}$  (sequence: KKAYV MLLPF FIGLL LGLIF GGAFW GPARH LKK) inserts spontaneously into lipid bilayers and has a dimerization affinity similar to that of GpA, which is known to form tight TM homodimers.<sup>5–7</sup> In addition, the lysine residues appended to both the N- and C-terminus greatly enhance the solubility of anti- $\alpha_{IIb}$  in water, allowing kinetic studies of membrane peptide folding starting from the aqueous phase. More importantly, the TM anti- $\alpha_{IIb}$  homodimers neither further aggregate to form higher-order oligomers or pores nor induce membrane lysis at lipid/peptide ratios of up to 10:1.<sup>6</sup> Thus, through the use of this peptide and an appropriate spectroscopic probe, it is possible to directly assess the time scales on which several important kinetic steps occur, including peptide binding to the membrane from aqueous solution, insertion into the membrane, and helix–helix association inside the membrane.

The peptide–membrane interaction was probed using either the native Trp fluorescence in anti- $\alpha_{IIb}$  or that arising from Phe<sub>CN</sub> in anti- $\alpha_{IIb}$ -Phe<sub>CN</sub>, an anti- $\alpha_{IIb}$  mutant wherein the Trp residue is replaced by Phe<sub>CN</sub>. It has been shown earlier that the Phe<sub>CN</sub> fluorescence is sensitive to its environment and thus can be used as a probe of protein conformation.<sup>8</sup> As Figure 1 shows, upon association of the respective peptides with 3:1 (w/w) POPC/POPG vesicles, both the Trp fluorescence and the Phe<sub>CN</sub> fluorescence increase, indicating the usefulness of these probes.

The peptide–membrane association kinetics were measured using a stopped-flow fluorescence technique.<sup>9</sup> Consistent with the equilibrium results (Figure 1), rapid mixing of anti- $\alpha_{IIb}$  and POPC/POPG vesicle solutions induces a time-dependent net increase in the Trp fluorescence, although some minor, wavy features occur in the late stages of the stopped-flow kinetics (Figure 2). Similarly, rapid mixing of anti- $\alpha_{IIb}$ -Phe<sub>CN</sub> with POPC/POPG vesicles also leads to an overall increase in the Phe<sub>CN</sub> fluorescence. However, the resultant stopped-flow kinetics clearly show three distinct phases

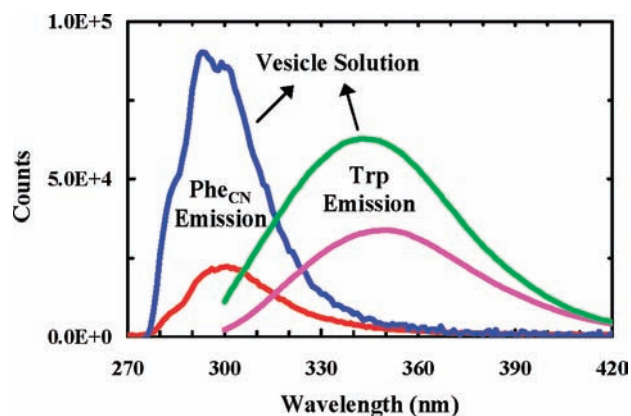


**Figure 1.** Fluorescence spectra of anti- $\alpha_{IIb}$  (pink and green) and anti- $\alpha_{IIb}$ -Phe<sub>CN</sub> (red and blue) in buffer and POPC/POPG vesicle solutions, as indicated. The peptide and lipid concentrations were 2.5  $\mu$ M and 0.86 mg/mL, respectively. The excitation wavelengths were 290 and 240 nm for anti- $\alpha_{IIb}$  and anti- $\alpha_{IIb}$ -Phe<sub>CN</sub>, respectively.

with alternating signs (Figure 2). Thus, these results not only underscore the importance of employing multiple probes in the study of complex “reaction” kinetics but also indicate that in the current case, the Phe<sub>CN</sub> fluorescence is more sensitive to those molecular events occurring during the time course leading to the formation of the TM anti- $\alpha_{IIb}$  homodimer.

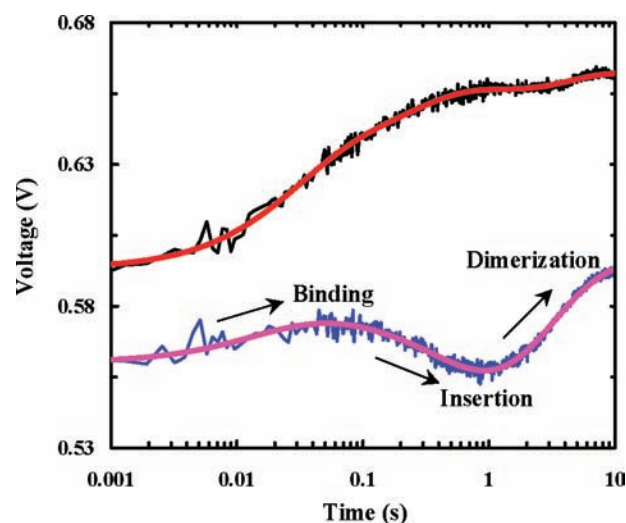


**Figure 2.** Stopped-flow kinetics of anti- $\alpha_{IIb}$  (black) and anti- $\alpha_{IIb}$ -Phe<sub>CN</sub> (blue) upon association with POPC/POPG vesicles (0.86 mg/mL). In both cases, the final peptide concentration was 2.5  $\mu$ M. The corresponding red and pink smooth lines are fits of these data to the model discussed in the text.

It is reasonable to assume that under the current experimental conditions, the peptides form TM homodimers as the reaction reaches

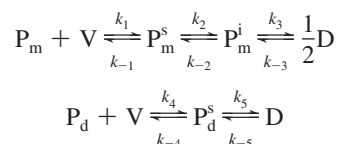
<sup>†</sup> Department of Chemistry, University of Pennsylvania.

<sup>‡</sup> Department of Biochemistry and Biophysics, University of Pennsylvania.

<sup>§</sup> University of Colorado.

equilibrium.<sup>5,6</sup> Therefore, similar to what is observed for many antimicrobial peptides,<sup>9,10</sup> the increase in Trp fluorescence in the early stages of the stopped-flow kinetics of anti- $\alpha_{\text{IIB}}$  most likely arises from the binding and insertion of the peptide into the membrane. However, a more insightful assessment of the entire kinetics reported by Trp fluorescence is less straightforward. On the other hand, the distinct features in the stopped-flow kinetics of anti- $\alpha_{\text{IIB}}$ -Phe<sub>CN</sub> make it relatively easier to interpret. It has been shown that upon burial in a hydrophobic environment, Phe<sub>CN</sub> fluorescence decreases.<sup>8</sup> Hence, it is reasonable to attribute the middle, negative kinetic phase to peptide insertion into the membrane, as such a process brings the Phe<sub>CN</sub> residue to the hydrophobic interior of the bilayer, and to attribute the initial, minor positive phase to membrane binding, as it brings the peptide to the polar head group region of the membrane. On the basis of these assignments and also the two-stage model of membrane protein folding,<sup>11</sup> it is logical to further attribute the third kinetic phase, in which the Phe<sub>CN</sub> fluorescence increases, to the formation of TM homodimers.

To provide quantitative information regarding the kinetics of membrane binding, insertion, and dimerization of anti- $\alpha_{\text{IIB}}$ , we fit all of the stopped-flow traces to the following kinetic scheme, which is a minimally expanded version of the two-stage model that includes peptide dimer formation in solution:



where P and V represent the peptide and vesicle, respectively, D represents the TM peptide dimer, the subscripts m and d refer to peptide monomer and dimer, respectively, and the superscripts s and i represent the surface-bound and membrane-inserted states of the peptide species, respectively. As shown in Figure 2, despite its lack of consideration of (a) the dynamic equilibria between the peptide monomer and dimer in solution and on the membrane surface and (b) the possibility that anti- $\alpha_{\text{IIB}}$  may form higher-order oligomers in solution, this simple model yields not only satisfactory fits to the anti- $\alpha_{\text{IIB}}$  and anti- $\alpha_{\text{IIB}}$ -Phe<sub>CN</sub> stopped-flow kinetics but also self-consistent kinetic and fluorescence parameters (Tables S1 and S2 in the Supporting Information). In addition, kinetic data obtained at other peptide concentrations (5  $\mu\text{M}$  for anti- $\alpha_{\text{IIB}}$  and 1, 5, and 15  $\mu\text{M}$  for anti- $\alpha_{\text{IIB}}$ -Phe<sub>CN</sub>) can also be fit by this model, yielding comparable microscopic rate constants but different percentages of P<sub>d</sub> in solution (Figures S1–S5 and Tables S1 and S2 in the Supporting Information), further substantiating the validity of the model.

Furthermore, and perhaps more importantly, the fitting parameters recovered also make physical sense. For example, all of the backward rate constants are negligible compared with the corresponding forward rate constants, indicating that all of the kinetic steps are essentially irreversible. This is consistent with previous thermodynamic measurements.<sup>5</sup> In addition, the recovered membrane binding rate constant is also in good agreement with those measured for other peptides,<sup>3,8,9</sup> and the membrane insertion rate constant of the anti- $\alpha_{\text{IIB}}$  monomer ( $2.4 \pm 0.7 \text{ s}^{-1}$ , the average of the  $k_2$  values in Table S1 in the Supporting Information), is very similar to that of the membrane pH (low) insertion peptide (pHLIP) ( $1.9 \text{ s}^{-1}$ ).<sup>12</sup> On the other hand, as expected, the membrane insertion rate constant of the anti- $\alpha_{\text{IIB}}$  dimer ( $0.5 \pm 0.1 \text{ s}^{-1}$ ) is close to that of a helical membrane protein, diacylglycerol kinase ( $\sim 0.24 \text{ s}^{-1}$ ).<sup>3</sup>

Moreover, our results indicate that the event of helix–helix association inside a membrane environment takes place on a time scale of a few seconds, which is not only much slower than the folding of the coiled-coil motif in solution<sup>13</sup> but also several orders

of magnitude slower than that expected for a diffusion-limited association process. The time scale of the latter is estimated to be on the order of a few hundreds of microseconds using the diffusion constant of a model TM peptide ( $3 \times 10^{-9} \text{ cm}^2 \text{ s}^{-1}$ )<sup>14</sup> and a two-dimensional random-walk model.<sup>15</sup> Taken together, these results thus indicate that the rate of TM helix–helix association is not diffusion-limited but rather is determined by the actual assembly process of the TM helical dimer, the folding of which requires proper backbone orientations and well-defined intermolecular side-chain–side-chain interactions.<sup>16</sup>

In summary, using two fluorescent amino acids, we were able to dissect the major kinetic events associated with the interaction of a designed TM peptide, anti- $\alpha_{\text{IIB}}$ , with a POPC/POPG model membrane, including membrane binding, insertion, and TM helix–helix association. While the kinetics of the latter process have been studied earlier, both in a micelle environment and via vesicle fusion,<sup>17</sup> the current study has allowed the direct assessment of the kinetics of this fundamental membrane folding event starting from the aqueous phase.

**Acknowledgment.** We thank the NIH (GM-065978, RR-01348) and the NSF (DMR05-20020) for funding.

**Supporting Information Available:** Materials and methods, stopped-flow kinetics at other peptide concentrations, and fitting parameters. This material is available free of charge via the Internet at <http://pubs.acs.org>.

## References

- (1) (a) Bogdanov, M.; Dowhan, W. *J. Biol. Chem.* **1999**, *274*, 36827–36830. (b) MacKenzie, K. R. *Chem. Rev.* **2006**, *106*, 1931–1977. (c) Stanley, A. M.; Fleming, K. G. *Arch. Biochem. Biophys.* **2008**, *469*, 46–66.
- (2) (a) Nagy, J. K.; Lonzer, W. L.; Sanders, C. R. *Biochemistry* **2001**, *40*, 8971–8980. (b) Otzen, D. E. *J. Mol. Biol.* **2003**, *330*, 641–649. (c) Allen, S. J.; Curran, A. R.; Templer, R. H.; Meijberg, W.; Booth, P. J. *J. Mol. Biol.* **2004**, *342*, 1279–1291.
- (3) Lorch, M.; Booth, P. J. *J. Mol. Biol.* **2004**, *344*, 1109–1121.
- (4) (a) Nymeyer, H.; Woolf, T. B.; Garcia, A. E. *Proteins* **2005**, *59*, 783–790. (b) Bond, P. J.; Sansom, M. S. P. *J. Am. Chem. Soc.* **2006**, *128*, 2697–2704. (c) Lopez, C. F.; Nielsen, S. O.; Srinivas, G.; DeGrado, W. F.; Klein, M. L. *J. Chem. Theory Comput.* **2006**, *2*, 649–655. (d) Bu, L.; Im, W.; Brooks, C. L. *Biophys. J.* **2007**, *92*, 854–863. (e) Chu, J. W.; Voth, G. A. *Biophys. J.* **2007**, *93*, 3860–3871. (f) Lee, J.; Im, W. *J. Am. Chem. Soc.* **2008**, *130*, 6456–6462.
- (5) Yin, H.; Slusky, J. S.; Berger, B. W.; Walters, R. S.; Vilaire, G.; Rustem, L. I.; Lear, J. D.; Caputo, G. A.; Bennett, J. S.; DeGrado, W. F. *Science* **2007**, *315*, 1817–1822.
- (6) Caputo, G. A.; Litvinov, R. I.; Li, W.; Bennett, J. S.; DeGrado, W. F.; Yin, H. *Biochemistry* **2008**, *47*, 8600–8606.
- (7) (a) Russ, W. P.; Engelman, D. M. *Proc. Natl. Acad. Sci. U.S.A.* **1999**, *96*, 863–868. (b) Adair, B. D.; Engelman, D. M. *Biochemistry* **1994**, *33*, 5539–5544.
- (8) (a) Tucker, M. J.; Oyola, R.; Gai, F. *Biopolymers* **2006**, *83*, 571–576. (b) Aprilakis, K. N.; Taskent, H.; Raleigh, D. P. *Biochemistry* **2007**, *46*, 12308–12313.
- (9) (a) Tucker, M. J.; Tang, J.; Gai, F. *J. Phys. Chem. B* **2006**, *110*, 8105–8109. (b) Tang, J.; Signarvic, R. S.; DeGrado, W. F.; Gai, F. *Biochemistry* **2007**, *46*, 13856–13863.
- (10) Constantinescu, I.; Lafleur, M. *Biochim. Biophys. Acta* **2004**, *1676*, 26–37.
- (11) Popot, J. L.; Engelman, D. M. *Biochemistry* **1990**, *29*, 4031–4037.
- (12) Tang, J.; Gai, F. *Biochemistry* **2008**, *47*, 8250–8252.
- (13) (a) Mo, J. M.; Holtzer, M. E.; Holtzer, A. *Proc. Natl. Acad. Sci. U.S.A.* **1991**, *88*, 916–920. (b) Wendt, H.; Berger, C.; Baici, A.; Thomas, R. M.; Bosshard, H. R. *Biochemistry* **1995**, *34*, 4097–4107. (c) Zitzewitz, J. A.; Bilsel, O.; Luo, J.; Jones, B. E.; Matthews, C. R. *Biochemistry* **1995**, *34*, 12812–12819.
- (14) Gambin, Y.; Lopez-Esparza, R.; Refay, M.; Sierrecki, E.; Gov, N. S.; Genest, M.; Hodges, R. S.; Urbach, W. *Proc. Natl. Acad. Sci. U.S.A.* **2006**, *103*, 2098–2102.
- (15) Tonegawa, Y.; Umeda, N.; Hayakawa, T.; Ishibashi, T. *Biomed. Res. Tokyo* **2005**, *26*, 207–212.
- (16) (a) DeGrado, W. F.; Gratkowski, H.; Lear, J. D. *Protein Sci.* **2003**, *12*, 647–665. (b) Bowie, J. U. *Nature* **2005**, *438*, 581–589. (c) Slivka, P. F.; Wong, J.; Caputo, G. A.; Yin, H. *ACS Chem. Biol.* **2008**, *3*, 402–411.
- (17) (a) Popot, J. L.; Gerchman, S. E.; Engelman, D. M. *J. Mol. Biol.* **1987**, *198*, 655–676. (b) Nannepaga, S. J.; Gawalapu, R.; Velasquez, D.; Renthal, R. *Biochemistry* **2004**, *43*, 550–559.

JA809007F